8th International Scientific – Technical Conference – PROCESS CONTROL 2008
June 9 – 12, 2008, Kouty nad Desnou, Czech Republic

WAVELET DE-NOISING IN IMAGE SEGMENTATION

GAVLASOVÁ ANDREA, PROCHÁZKA ALEŠ
Department of Computing and Control Engineering
Institute of Chemical Technology Prague, CZ
Email: andrea.gavlasova@vscht.cz

Abstract: Segmentation techniques include many methods which form a fundamental of image regions recognition and classification. The paper is devoted to the image segmentation using different methods and to comparison of their robustness with respect to various levels of noise. Proposed de-noising procedures are based upon appropriate thresholding of wavelet transform coefficients evaluated by selected decomposition functions. Resulting methods are verified for simulated images and then applied for selected MR biomedical images containing different structures. Sensitivity of segmentation to image components illumination, scale, translation and rotation is mentioned as well.

Keywords: Image de-noising, Discrete wavelet transform, Thresholding, Image segmentation, Watershed transform, Regions recognition

1 INTRODUCTION

Image segmentation techniques include many methods which form a fundamental of image regions recognition and classification. This contribution is devoted to the image segmentation using different methods and to comparison of their robustness with respect to various levels of noise. Appropriate image preprocessing procedures to reduce undesirable noise and spurious image artifacts are proposed at first. For this purpose the discrete wavelet transform (DWT) with three different wavelet functions, namely Haar, Daubechies4 and Daubechies8, is used. After wavelet decomposition appropriate thresholding of wavelet coefficients is evaluated followed by wavelet reconstruction using modified coefficients. Resulting filtered images are then segmented using two segmentation techniques: region growing (region-based technique) and watershed transform combined with distance transform (hybrid technique) [Jia-xin and Sen, 2005], [Gavlasová et al., 2008], [Rangayyan, 2005], [Gonzales et al., 2004]. Segmentation techniques are also applied to noisy images before their preprocessing. Finally the results after segmentation of noisy and preprocessed images are compared.

2 IMAGE DE-NOISING

Reduction of noise and spurious artifacts is an important preprocessing step. Within this context the *Discrete Wavelet Transform* (DWT) is used as a very efficient tool whose main benefit is in multi-resolution time-scale analysis ability.

2.1 Wavelet Functions

Wavelet functions used for signal and image analysis are derived from the initial (mother) function $h(t)$

$$h_{a,b}(t) = \frac{1}{\sqrt{a}}\, h\left(\frac{1}{a}\,(t-b)\right) \tag{1}$$

forming basis for the set of functions dilated by value $a = 2^m$ and translated by constant $b = k\,2^m$ for integer values of m, k.

Wavelet dilation closely related to spectrum compression according to Fig. 1 enables local and global signal and image analysis with different resolution levels. The one level image wavelet transform presented in Fig. 2 consists of:

(i) *The decomposition stage*: at first columns of matrix $\mathbf{A_{i,j}}$ are convolved with low-pass and high-pass filters and then the rows are down-sampled (keeping even indexed rows only). Then the rows of each of those 2 previous matrices are convolved with same filters and the columns

are down-sampled (keeping even indexed columns only). The decomposition stage results in this way in four images representing all combinations of low-pass and high-pass initial image matrix processing.

(ii) *The reconstruction stage*: at first rows are up-sampled and convolved with reconstruction filters and the corresponding images are summed. Then the columns of each matrix obtained are up-sampled again, convolved with reconstruction filters and summed to get final image of the original size.

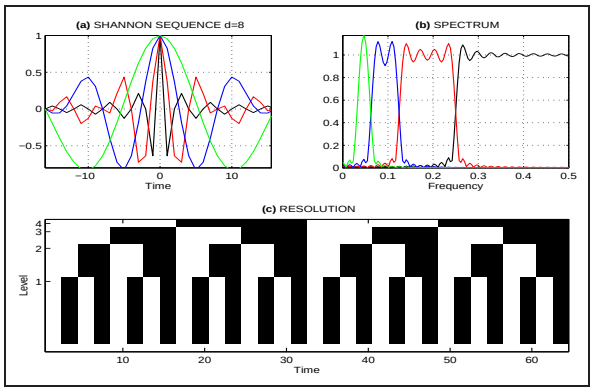

Figure 1 – Wavelet analysis presenting **(a)** the set of selected (Shannon) wavelet functions, **(b)** the effect of wavelet function dilation to its spectrum compression, and **(c)** localisation of wavelet transform coefficients in the time-scale space

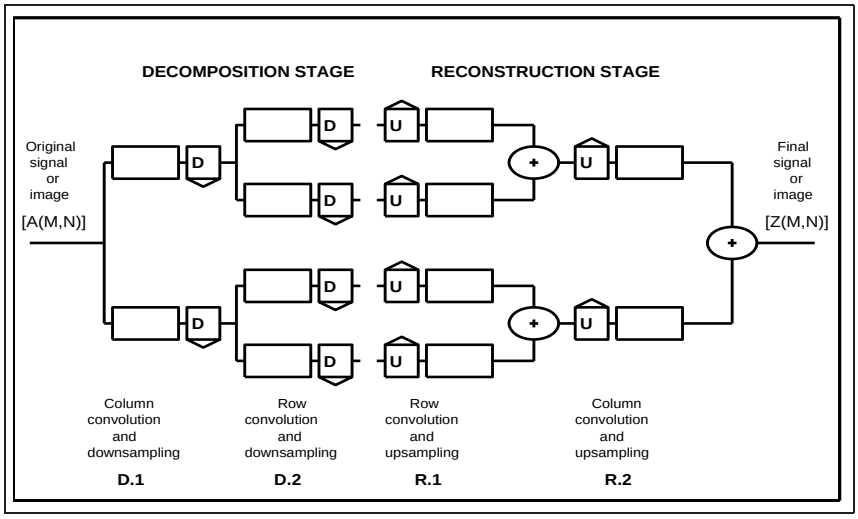

Figure 2 – Wavelet transform principle presenting **(D.1, D.2)** one level of image decomposition and **(R.1, R.2)** image reconstruction

2.2 Thresholding

Image de-noising can be achieved by appropriate thresholding of wavelet coefficients. In this case global hard-thresholding is used. It is possible to evaluate new coefficients $\overline{c}(k)$ using original coefficients $c(k)$ for a chosen threshold value δ by relation

$$\overline{c}(k) = \begin{cases} c(k) & \text{if } |c(k)| \geq \delta \\ 0 & \text{if } |c(k)| < \delta \end{cases} \tag{2}$$

This approach can be exploited for both signals and images using different methods of threshold level estimation.

3 IMAGE SEGMENTATION

Detection of regions of interest is an important step for most techniques of image analysis. Image segmentation using computers requires an algorithm for image pixels value analysis. These are then connected based on same regions features and information. Image segmentation techniques may be classified into four main categories [Rangayyan, 2005]:

- *thresholding techniques* - threshold determination based upon the valleys in the histogram of the image [Petrou and Bosdogianni, 1999]
- *boundary-based methods* - detection of intensity discontinuities lying at the boundaries (through gradient methods)
- *region-based methods* - assuming that neighboring pixels have similar values - region splitting, merging, region growing
- *hybrid techniques* - combination of boundary and region criteria for example applying watershed transform to a gradient image

3.1 Watershed Segmentation

The watershed transform is useful for many different image segmentation applications. In geographical sense *watershed* represents *watershed ridge lines* and *catchment basins* as we can see on Fig. 3. *Watershed ridge line* means in this sense points at which a drop of water can fall to more than one minimum and *catchment basin* means points from which a drop of water falls to a single minimum only.

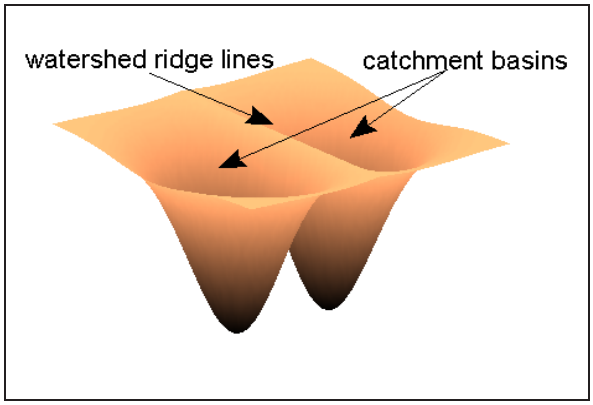

Figure 3 – Geographical sense of watershed transform

The *distance transform* is the common tool used together with the watershed transform. The distance transform of a binary image is a relatively simple concept [Gonzales et al., 2004]. Transformation of the binary image $\mathbf{A_{M,N}}$ is computed as Euclidean distance of each pixel $a_{i,j}$ to the nearest pixel $a_{k,l}$ with the value 1. Resulting matrix $\mathbf{B_{M,N}}$ is then formed by elements

$$b_{i,j} = \begin{cases} 0 & \text{for } a_{i,j} = 1 \\ \min\limits_{\forall k,l, a_{k,l}=1} \left(\sqrt{(i-k)^2 + (j-l)^2} \right) & \text{for } a_{i,j} = 0 \end{cases} \tag{3}$$

for $i = 1, 2, \cdots, M$, $j = 1, 2, \cdots, N$. An example of the application of the distance transform defined by Eq. (3) applied to matrix **A** results in the following matrix **B**.

1	1	0	0	0
1	1	0	0	0
0	0	0	0	0
0	0	0	0	0
0	1	1	1	0

Binary image A

0.00	0.00	1.00	2.00	3.00
0.00	0.00	1.00	2.00	3.00
1.00	1.00	1.41	2.00	2.24
1.41	1.00	1.00	1.00	1.41
1.00	0.00	0.00	0.00	0.00

Transformed image B

To use the distance transform we have to convert the original gray-scale image to binary image at first using optimal global image threshold by the Otsu's method [The Mathworks, 1993–2006]. In the next step image complement is defined. This image is then transformed using Eq. (3) and normalized. Image transform using the watershed method should be then applied to gray-scale image, where values of $f(x, y)$ are interpreted as heights. Detected image regions after watershed transform are then filled and connected components are labeled. At last the labeled image is normalized and we can calculate number of regions of interest.

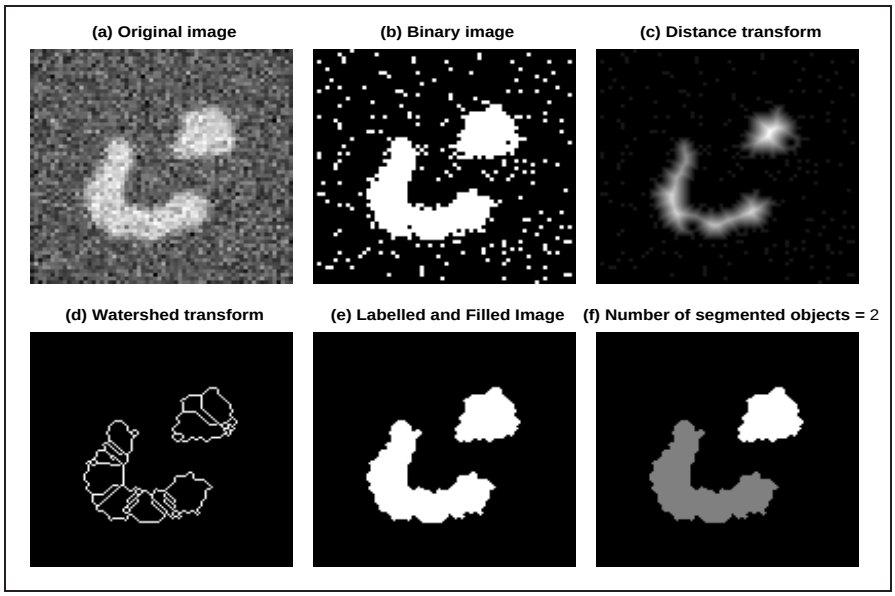

Figure 4 – Watershed segmentation presenting **(a)** original image, **(b)** binary image after thresholding, **(c)**, **(d)** results after the distance and watershed transform followed by **(e)** their labeling and **(f)** normalization

3.2 Region Based Segmentation

This segmentation technique is based on finding the regions directly and partitions matrix $\mathbf{A}$ into n subregions $\mathbf{A_1}, \mathbf{A_2}, \ldots, \mathbf{A_n}$ such that [Gonzales et al., 2004]

(a) $\bigcup_{i=1}^{n} \mathbf{A_i} = \mathbf{A}$

(b) $\mathbf{A_i}\ is\ a\ connected\ region,\ i = 1, 2, \ldots, n$

(c) $\mathbf{A_i} \bigcap \mathbf{A_j} = \emptyset\ \forall i, j,\ i \neq j$

(d) $\mathbf{P}(\mathbf{A_i}) = TRUE\ for\ i = 1, 2, \ldots, n$

(e) $\mathbf{P}(\mathbf{A_i} \bigcup \mathbf{A_j}) = FALSE\ for\ any\ adjacent\ regions\ \mathbf{A_i}\ and\ \mathbf{A_j}$

Region-based methods rely on the assumption that neighboring pixels within a region have similar values. Among these methods *the region growing algorithm* belongs.

Region growing is a procedure that groups pixels or subregions into larger regions based on predefined criteria for the growth. We start with a set of *seed points* and from these regions grow by appending to each seed those neighboring pixels that have predefined properties similar to the seed.

Algorithm:

- from the histogram of original image $\mathbf{I}$ the global threshold $\mathbf{T_g}$ is computed and significant thresholds are determined by user and saved as scalar $\mathbf{S_1}$
- the image with seed points **SI** is defined such that all the points in $\mathbf{I}$ with the same value as values in $\mathbf{S_1}$ become seed points
- testing (using global threshold $\mathbf{T_g}$) whether pixels of the image $\mathbf{I}$ are sufficiently similar to the seed values in $\mathbf{S_1}$

- the output is the segmented image where regions holes are filled followed by labeling each region with an integer value
- finally the labeled image is normalized and displayed

The substantial part of algorithm presented in Fig. 5 illustrates region growing method with defining seed points and labeling image according to Fig. 6:

- *Loading of image.*
```
I = load('SimImageNoised.mat'); I2=double(I);
```
- *Global threshold Tg of histogram.*
```
[n,xout]=hist(I2); T = iterative_thresh(I2);
Tg = (max(I2(:))  - T);
```
- *User defined thresholds in S1 and image with seed points SI.*
```
S1=input('Type the value(s) of important valleys in the
histogram:  ');
SIs=false(size(I2));
for i=1:length(S1), SI=I2==S1(i); SIs= SIs | SI; end
SI=SIs;
```
- *Testing: absolute value of difference between I2 and each seed point in SI must be* $\leq$ *Tg.*
```
TI=false(size(I2));
for l=1:length(S1), seedval=S1(l);
S=(abs(I2-seedval)<Tg); TI= TI | S; end
```
- *Image reconstruction and labeling.*
```
IR=imreconstruct(SI,TI);
Bw1=imfill( IR,'holes'); [L,num]=bwlabel(Bw1,8);
```

Figure 5 – Algorithm for region growing

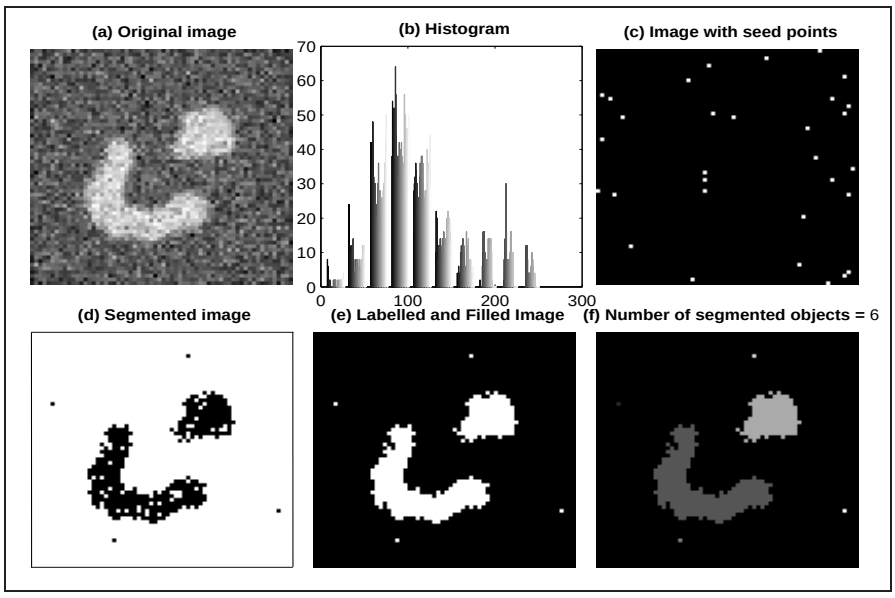

Figure 6 – Region growing method presenting **(a)** original image, **(b)** its histogram, **(c)** image with seed points after significant thresholds determination, **(d)** segmented image, **(e)** filled and labeled image and **(f)** normalized image

4 RESULTS

The segmentation methods using watershed transform and region growing algorithm were applied to the two testing images and one real MR biomedical image of backbone. The application of segmentation was divided to two parts yet: segmentation before and after image preprocessing. Image preprocessing is ensured by one level image wavelet decomposition using different wavelet functions followed by image reconstruction using modified wavelet coefficients.

4.1 Before Preprocessing

The images in the **(1.row)** in Fig. 7 were noised by adding Gaussian white noise with mean value 0.05 and variance 0.05. To these images were applied segmentation techniques and the results with number of segmented regions of interest are presented in Fig. 7.

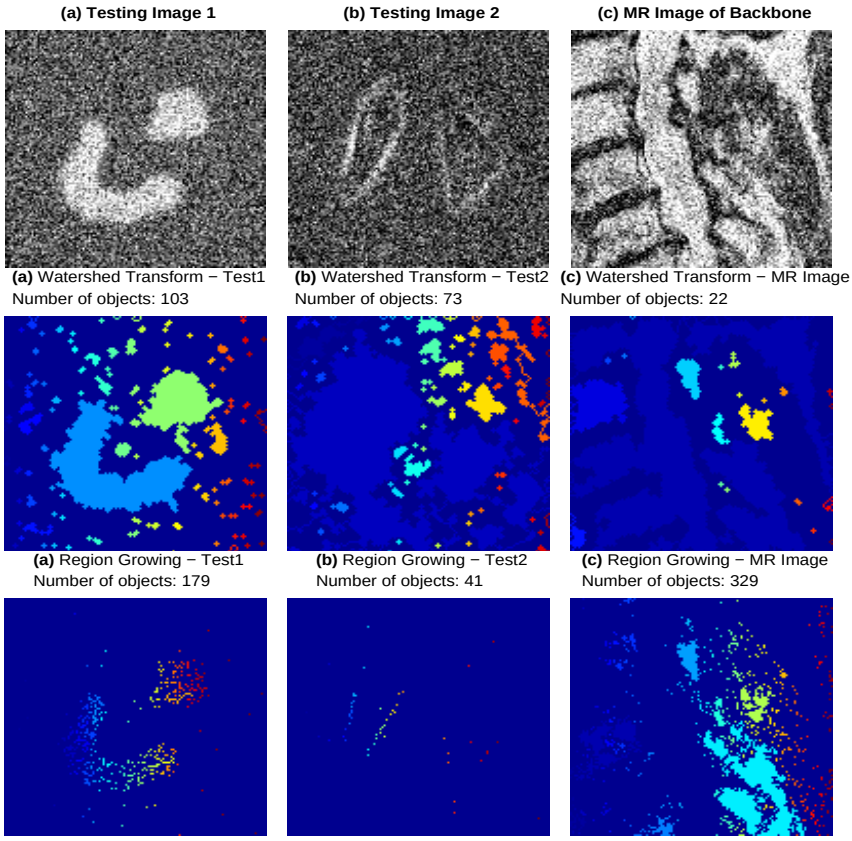

Figure 7 – Segmentation results of non-preprocessed images presenting at **(1.row)** original noised images, **(2.row)** segmentation after watershed transform and **(3.row)** region growing method

From Fig.7 and Tab.1 is obvious that watershed segmentation is more efficient. Although there are detected spurious artifacts, we can see in the **(2.row)**, the main ROIs are for the most part detected successfully. We can't tell it about results after region growing algorithm **(3.row)**. ROIs are detected, but they are composed of dozens more small segments.

Table 1 – Hit rate of ROIs after watershed (WST) and region growing (RG) noisy images segmentation

	Segmentation of Noisy Images				
	Number of ROIs	ROIs after WST	Hit rate (%)	ROIs after RG	Hit rate (%)
Test 1	**2**	103	19.4	179	1.12
Test 2	**2**	73	2.74	41	4.88
MR Image	**11**	22	50	179	6.15

4.2 After Preprocessing

In this stage was each input (Test 1, Test 2, MR Image) noisy image preprocessed by 1. level wavelet transform using Haar, Daubechies4 and Daubechies8 wavelet functions and subsequently was applied to de-noised images both watershed transform (Fig.8) and region growing algorithm (Fig.9). The results after image segmentation preprocessed by Haar wavelet transform at **(1.row)**, Daubechies4 wavelet transform at **(2.row)** and Daubechies8 wavelet trasnform at **(3.row)** are presented in Figs 8, 9 and Tables 2, 3.

4.2.1 Watershed segmentation

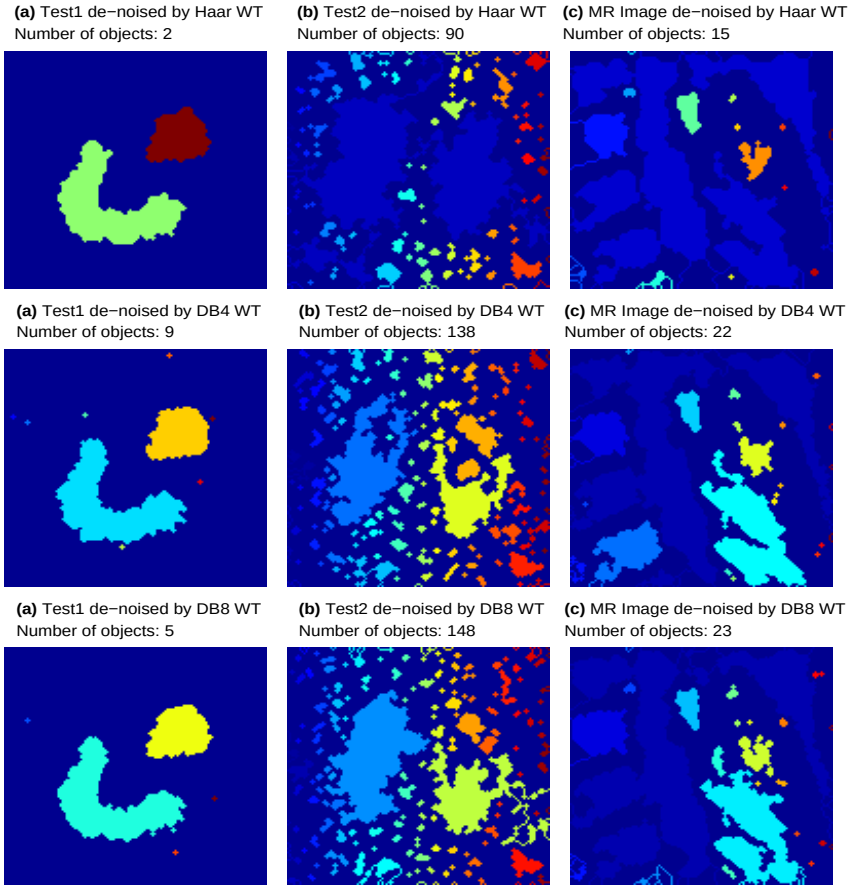

Figure 8 – Watershed segmentation results after image preprocessing using at **(1.row)** Haar wavelet decomposition into 1.level, **(2.row)** Daubechies4 wavelet decomposition into 1.level and **(3.row)** Daubechies8 wavelet decomposition into 1.level

Table 2 – Hit rate of regions of interest after application of watershed segmentation to preprocessed images decomposed by Haar, Daubechies4 and Daubechies8 wavelet functions

	Segmentation of De-noised Images						
	Number of ROIs	ROIs after Haar	Hit rate (%)	ROIs after DB4	Hit rate (%)	ROIs after DB8	Hit rate (%)
Test 1	**2**	2	100	9	22.22	5	40
Test 2	**2**	90	2.22	138	1.45	148	1.35
MR Image	**11**	15	73.3	22	50	23	47.8

4.2.2 Region growing segmentation

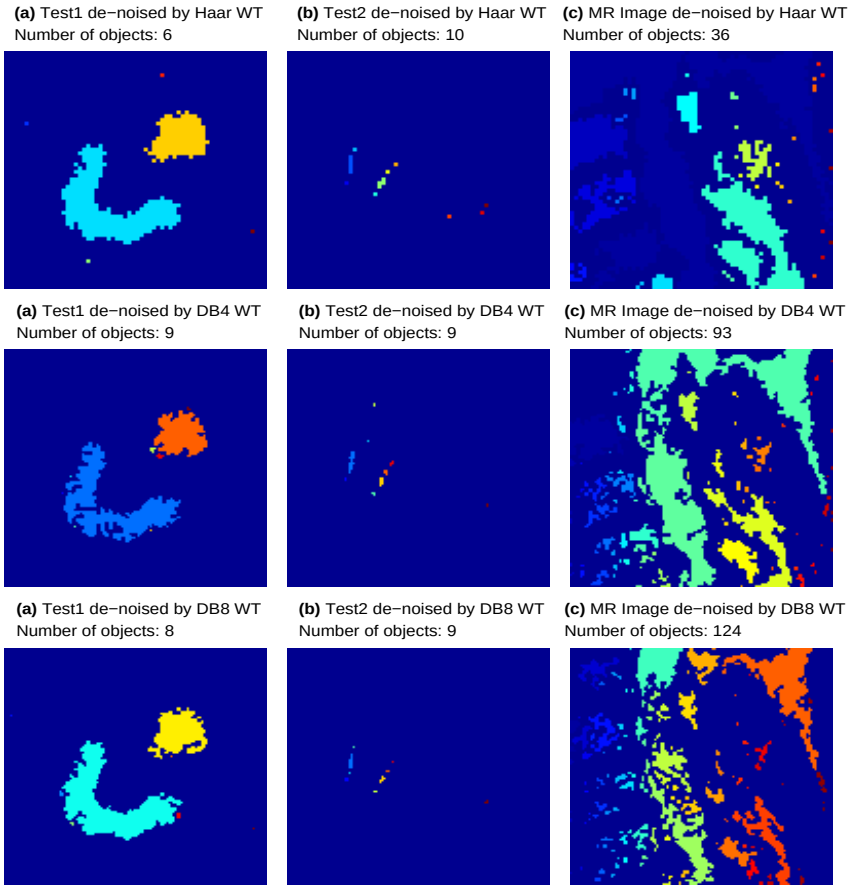

Figure 9 – Region growing segmentation results after image preprocessing using at **(1.row)** Haar wavelet decomposition into 1.level, **(2.row)** Daubechies4 wavelet decomposition into 1.level and **(3.row)** Daubechies8 wavelet decomposition into 1.level

Table 3 – Hit rate of regions of interest after application of region growing method to preprocessed images decomposed by Haar, Daubechies4 and Daubechies8 wavelet functions

	Segmentation of De-noised Images						
	Number of ROIs	ROIs after Haar	Hit rate (%)	ROIs after DB4	Hit rate (%)	ROIs after DB8	Hit rate (%)
Test 1	**2**	6	33.3	9	22.22	8	25
Test 2	**2**	10	20	9	22.22	9	22.22
MR Image	**11**	36	30.6	93	11.8	124	8.9

5 CONCLUSIONS

The paper presents the use of the two selected segmentation techniques in dependence on level of noise. The resulting figures and tables prove that the watershed segmentation is more efficient in the case of both noisy images and de-noised images. In the case of segmentation after preprocessing the connection of Haar wavelet transform followed by watershed segmentation seems to be the most efficient.

Another extension of this study could be in monitoring of fruitfulness segmentation depending on the selected level of image wavelet decomposition followed by different methods of thresholding.

Further studies will be devoted to studies of specific segmentation techniques and sensitivity of segmentation to image components illumination, scale, translation and rotation.

6 ACKNOWLEDGEMENTS

This work has been supported by the Ministry of Education of the Czech Republic (program No. MSM 6046137306). All MR images were kindly provided by the Neurocenter Caregroup.

References

GAVLASOVÁ, A.; PROCHÁZKA, A.; POŽIVIL, J.; VYŠATA, O. 2008. Functional transforms in mr image segmentation. In *ISCCSP2008*, 1357–1360. 445 Hoes Lane Piscataway NJ 08854-4150 USA: IEEE Operations Center.

GONZALES, R. C.; WOODS, R. E.; EDDINS, S. L. 2004. *Digital Image Processing Using Matlab*. Upper Saddle River New Jersey 07458: Pearson Prentice Hall. ISBN 0-13-008519-7, 609 pp.

JIA-XIN, C.; SEN, L. 2005. A medical image segmentation method based on watershed transform. In *IEEE CIT'05*.

PETROU, M.; BOSDOGIANNI, P. 1999. *Image Processing: The Fundamentals*. Baffins Lane Chichester West Sussex P019 1UD England: John Wiley and Sons Ltd. ISBN 0-471-99883-4, 333 pp.

RANGAYYAN, R. M. 2005. *Biomedical Image Analysis*. 2000 N.W. Corporate Blvd. Boca Raton, Florida 33431: CRC Press LLC. ISBN 0-8493-9695-6, 1272 pp.

THE MATHWORKS, I. 1993–2006. *Image Processing Toolbox User's Guide*. 3 Aplle Hill Drive, Natick, MA 01760-2098, 5 edition.